Oceanologia 64 (2022) 35—49

Available online at www.sciencedirect.com

ScienceDirect

journal homepage: www.journals.elsevier.com/oceanologia

ORIGINAL RESEARCH ARTICLE

A comparative study of biosynthesized marine natural-product nanoparticles as antifouling biocides

Khaled Mahmoud Abdelsalam[a,*], Nayrah Aly Shaltout[b], Hassan Abduallah Ibrahim[c], Hermine Ramzy Zaki Tadros[b], Mohamed Abd-Elnaby Aly-Eldeen[b], Ehab Aly Beltagy[c]

[a] *Taxonomy & Biodiversity of Aquatic Biota Lab, National Institute of Oceanography and Fisheries, NIOF, Cairo, Egypt*
[b] *Marine Chemistry Lab, National Institute of Oceanography and Fisheries, NIOF, Cairo, Egypt*
[c] *Microbiology Lab, National Institute of Oceanography and Fisheries, NIOF, Cairo, Egypt*

Received 15 December 2020; accepted 21 August 2021
Available online 10 September 2021

KEYWORDS
Antifouling;
Nanoparticles;
Chitosan;
Ulva fasciata;
Avicennia marina leaves

Abstract In this study, biosynthesized nanoparticles using chitosan, *Ulva fasciata*, and *Avicennia marina* leaves extracts (A, B, and C, respectively), were evaluated as paint additives to control marine fouling on different substrates. These biocidal nanoparticle compounds were prepared using a green biosynthesis method. Their characterizations were conducted using Fourier-Transform Infrared spectroscopy and Transmission electron microscopy. Each nanoparticle compound was mixed with a prepared paint, resulting in three formulations for each (e.g. 1C, 2C, 3C), containing 20%, 40%, and 60% by weight. Painted PVC, wood, and steel with these nine paints, and the control were immersed in seawater for different periods. After two months of immersion, the least number of fouling species, (one species) was recorded on both the wood and steel panels that were coated with paint (1C). Meanwhile, after four months, the least numbers of fouling (four and six species) were recorded on wood and steel panels that were coated with paint (3C). After around seven months of immersion, the least numbers

* Corresponding author at: National Institute of Oceanography and Fisheries, NIOF, Cairo, Egypt. Tel. +2 03 4801553; fax: +2 034801499.
E-mail addresses: kh.abdelsalam@gmail.com (K.M. Abdelsalam), nshaltout@gmail.com (N.A. Shaltout), drhassan1973@yahoo.com (H.A. Ibrahim), herminetadros@gmail.com (H.R.Z. Tadros), m_niof@yahoo.com (M.A.-E. Aly-Eldeen), ehab.beltagy@gmail.com (E.A. Beltagy).
Peer review under the responsibility of the Institute of Oceanology of the Polish Academy of Sciences.

Production and hosting by Elsevier

https://doi.org/10.1016/j.oceano.2021.08.004

of fouling species (five and ten) were recorded on wood and steel panels that were coated with paints (1C and 3C), respectively. The steel panel coated with (3C), harbored ~2% of the total number of barnacles found on the control, after 7 months of immersion. The superior antifouling agent efficiency of extract (C) nanoparticles can be attributed to its constituents of polyphenols, ammonium compounds, and high concentrations of alcohols, besides the presence of both aromatic and aliphatic amide and amide derivatives.

1. Introduction

In the marine environment, the surface of any submerged substratum is covered by the microbial colonizers which, form complex biofilms composed of bacteria, archaea, fungi, protozoa, and unicellular microalgae (Dobretsov and Rittschof, 2020). Biofilms could impact the larvae of marine invertebrates (macro-fouling) in their selection of suitable substrates on which to settle and metamorphose (Hadfield 2011; Peng et al., 2020).

Marine biofouling has spawned a billion-dollar industry, where biocides, cleaners, and antifouling materials are required globally to prevent their formation. on the other hand, green chemistry has been evolved as an alternative to the use of environmentally harmful processes and products due to the serious consequences that the world is facing (De Marco et al., 2019; Hurst, 2020), and the development of efficient and environmentally friendly antifouling compounds has become of pressing interest for marine coating businesses (Wang et al., 2017).

Marine macroalgae are widely perceived to be makers of a broad spectra of biogenic compounds, including polyunsaturated fatty acids, flavonoids, terpenoids, alkaloids, quinones, sterols, polyketides, phlorotannins, polysaccharides, glycerols, peptides, and lipids (Mohy El-Din and El-Ahwany, 2015) which have strong activities, for example, as antifouling (Bhadury and Wright, 2004), antimicrobial (Zbakh et al., 2012), and anticoagulant agents (Kolanjinathan et al., 2014; Shi et al., 2008).

Also, chitosan has been shown to be biocompatible, biodegradable, and non-toxic, making it suitable for a wide range of uses in the pharmaceutical industry (Puvvada et al., 2012; Tikhonov et al., 2006). Moreover, it has been widely used as an antimicrobial agent against fungi, viruses, and bacteria (Kong et al., 2010). Recently, metallic nanoparticles are the alternative in biological and scientific challenges in different fields of science (Patil and Kim, 2017, 2018; Shah et al., 2015). Nanoscale materials have emerged as novel antimicrobial agents owing to their high surface area-to-volume ratio, which increases their contact with microbes, hence increasing their ability to permeate cells (Lamsal et al., 2011).

Biological synthesis is a reliable production method of metal nanoparticles. For example, Silver nanoparticles (Ag-NPs), was one of the most widely used agent that have antifouling activity due to their size, shape, and applications (Krishnan et al., 2015). By using an aqueous extract of the green seaweed *Ulva* (*Enteromorpha*) *compressa* as a reductant and a stabilizing agent, (Ramkumar et al., 2017) synthesized biocompatible silver nanoparticles. They indicated that metal nanoparticles synthesized by macroalgae could potentially be utilized in antifouling applications.

Given this background, the present study evaluates the effect of biosynthesized chitosan nanoparticles as well as biosynthesized iron nanoparticles capped with *Ulva fasciata* and mangrove leaf extracts, mixed in three different weight ratios with a prepared paint formulation and resulting in nine paints on biofilm formation on different surfaces for the control of marine fouling. Moreover, it targets to compare between different concentrations of the biosynthesized nanoparticles of various extracts, aiming to determine the most suitable extract concentration in the prepared paint formulation that will give the maximal antifouling activity.

2. Material and methods

2.1. Medium

A nutrient agar medium comprising 5 g peptone, 10 g yeast extract, and 15 g agar was prepared using 1-L seawater for the counting of marine viable heterotrophic bacteria and for detecting antibacterial activity.

2.2. Collection of mangrove plant samples

In April 2017, fresh mangrove leaves (*Avicennia marina*) were collected from the Safaga coastal area (26°35′42″N, 34°01′13″E) of the Red Sea, Egypt. The gathered sample leaves were washed using water from a faucet, and then with distilled water, to remove any adhering salt and other associated creatures. The leaves were dried in the shade, and then ground and powdered.

2.3. Collection of algal samples

In April 2017, fresh *U. fasciata* samples were collected from the Abu Qir Bay region (31°16′27″N, 30°07′16″E) of the Mediterranean Sea, Egypt. In the laboratory, the algae were washed using water from a faucet, to eliminate any remaining impurity and epiphyte. Microscopic identification of the investigated algae was carried out according to (Abdel Aleem, 1993).

2.4. Biosynthesis of iron nanoparticles

Around 10 g of finely cut *A. marina* leaves or *U. fasciata* were added to 100 mL of distilled water, and the mixture was boiled for 1 h. The resulting solution was filtered

through a Whatman no. 1 filter paper. A total of 10 mL of the collected filtrate was treated with 90 mL of an aqueous solution of iron chloride (0.001 M $FeCl_3$), and then stirred for 2 h, resulting in the formation of a brownish solution, which indicated the formation of iron nanoparticles.

2.5. Preparation of chitosan nanoparticles

In the present study, a chitosan compound namely [Poly (beta-(1,4)-2-amino-2-deoxy-D-glucose) Poly(beta-(1,4)-D-glucosamine] was used. The low molecular weight chitosan nanoparticles were prepared according to a method reported by (Tang et al., 2007). Briefly, 20 mg of chitosan was dissolved in 40 mL of 2.0% (v/v) acetic acid. Then, 20 mL of 0.75 mg/mL sodium tripolyphosphate was slowly dropped into the solution, with stirring. The chitosan nanoparticle suspension was collected and stored in deionized water. The supernatant was discarded and the chitosan nanoparticles were air-dried prior to further use and analysis.

2.6. Characterization of the biosynthesized nanoparticles

2.6.1. Fourier-transform infrared (FTIR) spectroscopy

Approximately 1 mL solution of the nanoparticles (diluted with 1:20 v/v Milli Q water) was centrifuged at 10 000 g for 10 min and their pellets were re-dispersed in sterile distilled water. This centrifugation and re-dispersion process was repeated three times to ensure the removal of any free biomass residue or compound that was not the capping ligand of the nanoparticles. Afterward, the purified suspension was freeze-dried to obtain a dry powdered sample. Finally, the dried purified nanoparticles as KBr pellets were analyzed using FTIR spectroscopy in the diffuse reflectance mode at a resolution of 4 cm^{-1} in the range of 4000—375 cm^{-1}, using a Thermo Nicolet AVATAR 300 FTIR spectrometer.

2.6.2. TEM analysis

The structure, size, and morphology measurements were conducted on the biosynthesized chitosan and iron nanoparticles using transmission electron microscopy (TEM, Jeol CX 100 — Eching b. München, Germany), in which a thin film of the sample placed on a gold-coated copper grid was used for capturing images of the nanoparticles.

2.7. Marine paint preparation

A marine paint formulation comprising 25 g of Linseed oil as a binder material, 10 g of iron oxide, 24 g of zinc oxide, 13 g of complementary pigment, and 38 g of xylene was prepared through careful blending of these paint ingredients using a ball mill. The three biosynthesized nanoparticles (chitosan, *U. fasciata*, and *A. marina*) were mixed with the paint composition in ratios of 20%, 40%, and 60%, (denoted as 1, 2, and 3, respectively), to produce nine marine paint formulations.

2.8. In situ experiments

In situ experiments were conducted in the Eastern Harbour of Alexandria, Egypt, to test the effectiveness of the paint formulations as antifouling agents. Three iron frames (each measuring 100 × 70 cm, carrying test panels) were dangled under the jetty of the National Institute of Oceanography and Fisheries. These frames were exposed to the marine environment for different periods (around two, four, and seven months). The test panels (4 × 10 cm) made from three types of substrates, PVC, wood, and steel (Figure 1) were treated using the modified paints. Wood and steel are the main building components used for producing both small and large ships, while PVC is a neutral or inert substrate, similar to the material used in the manufacture of fiber glass boats. The panels were tightly fixed to each iron frame using thin silk ropes at both ends of the panel.

2.9. Preparation of the test panels prior to application of the paint

In this study, iron frames, holding 36 test panels, were used, of which 12 were made from PVC, 12 from wood, and 12 from steel. Each set of 12 panels comprised three control (untreated) panels and three sets of samples of modified paint with different active nanoparticles, with each sample containing three concentrations, 20%, 40%, and 60%, of each nanoparticle material in the paint composition. Before applying paint to the surfaces of the wood and steel panels, they were first polished using different grades of emery papers and cleaned using xylene.

2.10. Immersion of the panels

The three iron frames were immersed in seawater on the same starting date, 27/11/2017. After three, six, and ten days of immersion, microbiological samples from all test panels of the three iron frames were respectively collected to estimate the total bacterial count of the biofilms formed. Afterward, the level of marine fouling was monitored on different test panels of the three iron frames with different immersion durations, and photographed. The iron frames were collected in the following order: iron frame I (collected on 05/02/2018 after immersion for more than 2 months), iron frame II (collected on 12/04/2018 after immersion for more than 4 months), and iron frame III (collected on 25/06/2018 after immersion for around 7 months).

2.11. Physicochemical parameter measurements of the seawater

The physicochemical parameters (temperature, salinity, pH, dissolved oxygen (DO) content, and PO_4^{3-}, SiO_3^-, NO_2^-, NO_3^-, and NH_3 concentrations) of the water in the Eastern Harbour of Alexandria, Egypt, were measured each time the panels were inspected or collected. The pH values of the water samples were estimated in situ using a pH meter (Orion Research model 210 digital pH meter). The DO content was measured using the Winkler method, modified by FAO (Food and Agriculture Organization) in 1975. The PO_4^{3-}, SiO_3^-, NO_2^-, NO_3^-, and NH_3 concentrations in each sample were determined colorimetrically according to a previously proposed method (Parsons et al., 1984) using a double-beam spectrophotometer (Shimadzu UV-150-02), with the values

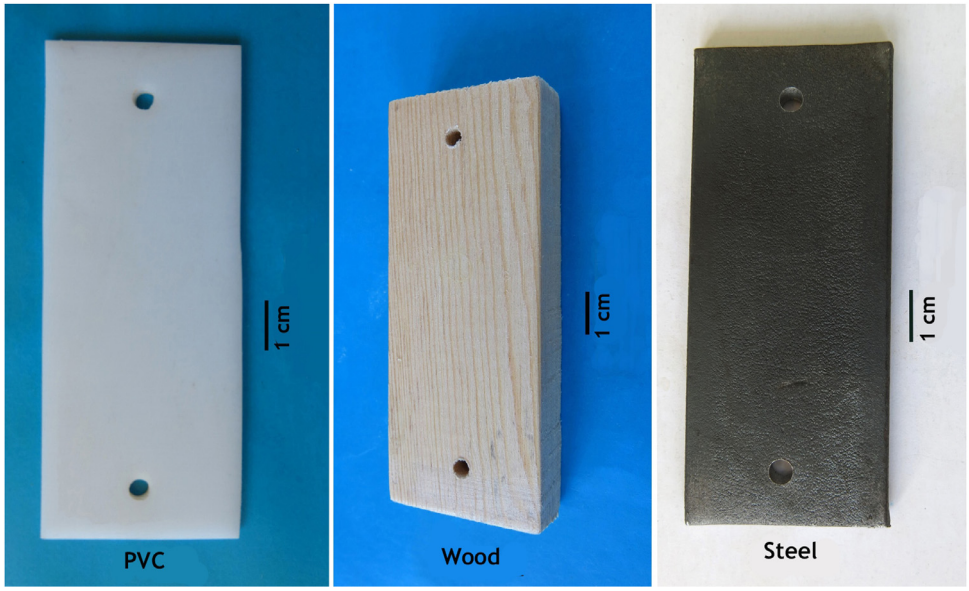

Figure 1 The three types of substrates used in the study.

expressed in μM. The sulfate (SO_4^{2-}) content of the samples was precipitated as barium sulfate, whose concentration was then measured turbidimetrically according to a previous method (Bather and Riley, 1954).

2.12. Microbiological investigation

2.12.1. Counting the bacteria that form the biofilms

Swabbing using sterile cotton toothpicks was carried out per cm^2 of the panels in duplicate, to determine the viable bacterial counts on the different materials that had been submerged in seawater. Each swab was then added to 1 mL of sterilized seawater and shaken well. Next, a portion (100 μL) from each sample was transferred to nutrient agar plates prepared with seawater to count the bacteria. The plates were incubated at 30°C for 24—48 h, after which bacterial counts were estimated (Abou-Elela, 1994).

2.12.2. Antibacterial activity of the biosynthesized nanoparticles

A well-cut diffusion technique was used to test how the different crude extracts inhibit the growth of the indicator bacteria. The nutrient agar medium (50 mL) inoculated with the test bacteria were poured into the nutrient agar plates. After the medium had solidified, wells were punched out using a 0.5-cm cork-porer. The test extracts (50 μL) were then transferred into each well. All plates were incubated at an appropriate temperature for 24—48 h, after which the radius of the clear zone around each well (Y) and the radius of the well (X) were linearly measured in mm, where dividing Y^2 by X^2 allowed the determination of the absolute unit (AU) of the clear zone. Thus, the AU of the crude extract was calculated according to the following equation: $AU = Y^2\pi / X^2\ \pi$ (Abdel-Latif et al., 2018).

2.13. Identification and estimation of the macro-fouling communities

In the laboratory, after the removal of the panels from the iron frames, each of them was photographed, and then preserved for careful inspection of the marine fouling species. Some relevant scientific publications were consulted for the identification of the species (Bellan-Santini et al., 1989; Campbell et al., 1982; Riedl, 1970; Zabala and Maluquer, 1988).

2.14. Statistical treatment

Data of marine fouling was treated with a two-way ANOVA test using SPSS software version (22). The number of recorded fouling species was used as a dependent variable meanwhile, durations and different concentrations of compounds as fixed factors. A *P*-value of <0.05 is considered as a significant value. A post hoc test using (Tukey HSD) was used to test if there is a mean difference among durations or between control and different concentrations of the paint compounds.

3. Results

3.1. Physicochemical parameters

Some physicochemical parameters of the Eastern Harbour water, at the site of the panel immersion, were measured when the panels were inspected or collected (Supplementary Table 1). According to the data obtained, all measured physicochemical parameters are within the normal range of those expected for water from the Mediterranean Sea. Moreover, the chemical parameters of the water do not show any sudden variation, indicating that the paints do not pollute the environment.

3.2. FTIR spectral analysis

FTIR spectroscopy is a useful tool for studying the non-centrosymmetric (IR active) modes of vibrations, which enable the determination of the secondary structure in nanoparticle—biomolecule interactions. In the current study, the results of FTIR analysis of the used biosynthesized nanoparticles are as follows:

3.2.1. Nano-chitosan

As shown in Figure 2a, the FTIR spectrum of nano-chitosan feature absorption bands closer to those of chitosan that have been reported previously by (Venkatesan et al., 2011), comprising carbonyl group (C=O, at 1740 cm^{-1}) and C—H stretching peaks at 1411 cm^{-1}. The peaks observed at 3190 cm^{-1} can be attributed to N—H and O—H stretching vibrations. The peak at 1533 cm^{-1} can be assigned to the N—H bending vibration of amide II, while that at 1379 cm^{-1} can be assigned to the $-CH_3$ symmetrical deformation mode (scissoring) of the amide group. The bands assigned to the stretching vibrations of C—O—C linkages in the polysaccharide structure appear at 1150 and 1063 cm^{-1}. The band at 1150 cm^{-1} corresponds to the anti-symmetric stretching of the C—O—C bridge. The peak at 2871.26 cm^{-1} corresponds to the methyl group (CH_3), while that at 2361.02 cm^{-1} represents the alkane group (CH). Two alkene (C=C) peaks can be observed at 1631.91 and 647.69 cm^{-1}, while the ether group (C—O—C) exhibits a peak at 1031.73 cm^{-1}.

These observed peaks represent the major functional groups of flavonoids, tri-terpenoids, and polyphenols. Hence, the terpenoids are proven to exhibit good activity in converting the aldehyde groups to carboxylic acids.

3.2.2. Iron nanoparticles biosynthesized using a *U. fasciata* extract

The FTIR spectrum of the FeNPs synthesized using the *U. fasciata* extract was used to identify the functional groups of the active components in the sample, based on the peak values. The results of the FTIR analysis (Figure 2b) show different peaks at 615.99 and 843.95 cm^{-1} for the functional group alkyl halides, while the peak at 928.98 cm^{-1} corresponds to the carboxylic acid functional group. In addition, the peaks at 1030.58 cm^{-1} represent aliphatic amines. The peak at 1442.14 cm^{-1} represents aromatic amines, while the recorded peak at 1631.71 cm^{-1} indicates amides. These strong peaks confirm the stretching vibrations of primary and secondary amines. Moreover, the peak at 2324.05 cm^{-1} represents the nitrile functional group, while the identified peak at 425.85 cm^{-1} corresponds to alcohols and phenols.

From the spectrum, hydroxyl, amino, and C—H group peaks can be observed in the region of 3000—3600 cm^{-1}, corresponding to the OH group of the monomeric hydrogen bond and phenol rings. C=C ring stretching can be observed at 2079.48 cm^{-1}. Overall, the peaks in this spectrum are characteristic of belonging to alginic acid, flavonoids, tannins, gallic acid, and other phenols. These soluble compounds act as reducing and stabilizing agents, preventing the aggregation of the nanoparticles in solution, explaining the high antibacterial activity of the material.

3.2.3. Iron nanoparticles biosynthesized using an *A. marina* leaf extract

FTIR spectroscopy measurements were conducted to identify the biomolecules responsible for the reduction of Fe^{3+} and capping of the bio-reduced FeNPs synthesized using mangrove leaf extract (Figure 2c). The spectrum shows a broad band at 3277 cm^{-1}, corresponding to the O—H stretching of a high concentration of alcohols or phenols. The band at 2924.69 cm^{-1} is attributable to the O—H stretching of carboxylic acids, while the weak-to-strong band at 1438.3 cm^{-1} corresponds to the C—C stretching of aromatic C=C.

Furthermore, the medium band at 1220.36 cm^{-1} is attributable to the C—O stretching of carboxylic acids. In addition, the multiple broad peaks at 2359.57 cm^{-1} correspond to the N—H stretching of ammonium ions, while the medium-intensity band at 1628.10 cm^{-1} corresponds to C=N stretching. The band at 1536 cm^{-1} can be assigned to the N—O stretching of nitro compounds. Moreover, the weaker band at 1373.90 cm^{-1} corresponds to the N—O stretching of amides. The broad band at 1023.87 cm^{-1} accounts for the C—X stretching of fluoroalkanes. The strong band at 775.90 cm^{-1} can be assigned to the C—H stretching of aromatic benzene. The amide group peaks confirm the presence of the enzymes responsible for the reduction and stabilization of the metal ions. The recorded polyphenols of the mangrove leaf extract are proved to be a potential reducing agent in the synthesis of silver nanoparticles (Qi et al., 2004).

Notably, the FTIR spectra for the *U. fasciata* and *A. marina* nano-extracts with iron show the efficient binding of several functional groups (alcohols, carboxylic acids, esters, and ethers) with metal to form iron nanoparticles. These groups have been previously proven to act as potential reducing agents of major chemical classes (flavonoids, triterpenoids, and polyphenols) during the synthesis of iron nanoparticles. It was confirmed from the N—H stretching vibration of the primary amines and C—N stretching, besides the overlapping of the aliphatic amines, that the metal is strongly bound, so secondary metabolites from *U. fasciata* and the *A. marina* leaves form a capping of iron nanoparticles to prevent particle agglomeration and stabilize them in the medium. These results provide good evidence of their high efficiency as antibacterial and antifouling agents.

3.3. TEM analysis

The TEM image of the chitosan nanoparticles shown in Figure 3a revealed that the diameters of the nanoparticles were in the range of 2.16—4.32 nm and that most of them were spherical, in accordance with the observations made by (Ali et al., 2011). The diameters of the iron nanoparticles biosynthesized using *U. fasciata* leaf and *A. marina* extracts were in the range 1.44—18.5 nm (Figure 3b and c). The type of extract used determines the shapes and diameters of each type of biosynthesized nanoparticles, i.e., they are dependent on the reducing agent, which differs according to the extract used (see the FTIR spectra). The extracted compounds from the selected *U. fasciata* and *A. marina* leaves served as reducing agents and efficient stabilizers (Mahdavi et al., 2013).

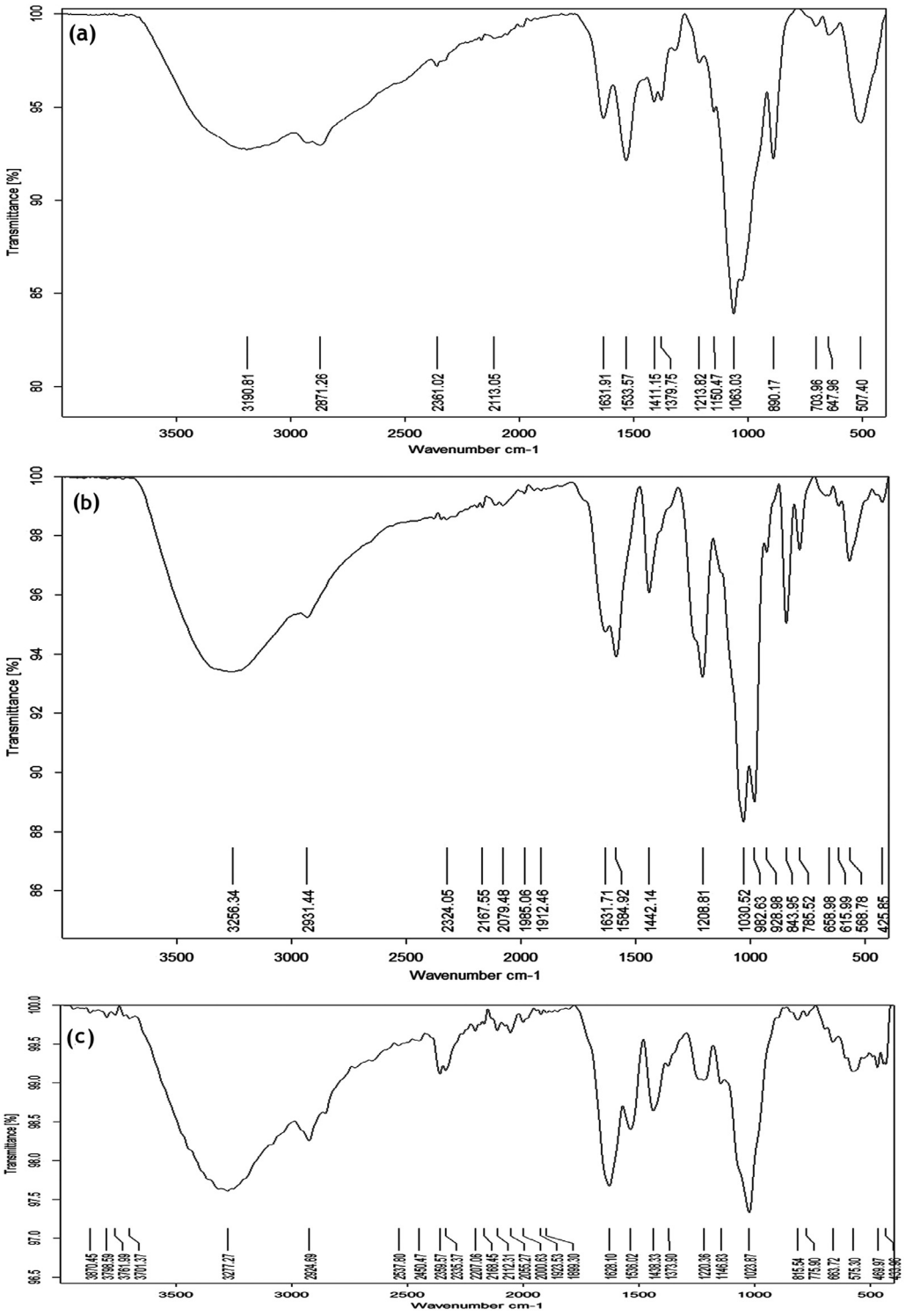

Figure 2 FTIR spectra of the (a) chitosan nanoparticles, (b) iron nanoparticles biosynthesized using a *Ulva fasciata* extract, and (c) iron nanoparticles biosynthesized using an *Avicennia marina* leaf extract.

3.4. Antibacterial activity of the crude extracts

The antibacterial activities of several crude extracts (*U. fasciata* and *A. marina*) and nanoparticle composites (chitosan) were screened against the bacterial community in seawater taken from the Eastern Harbour of Alexandria, Egypt, and then compared with the reference strains *Escherichia coli* ATCC 19404 and *Staphylococcus aureus* ATCC 6538. However, the data shown in Table 1 indicate that the *A. marina* (leaf extract only) has no AUs against both bacterial community and *E. coli*, while, it shows low AU (1.8) against *S. aureus*. Also, the chitosan composite exhibits the

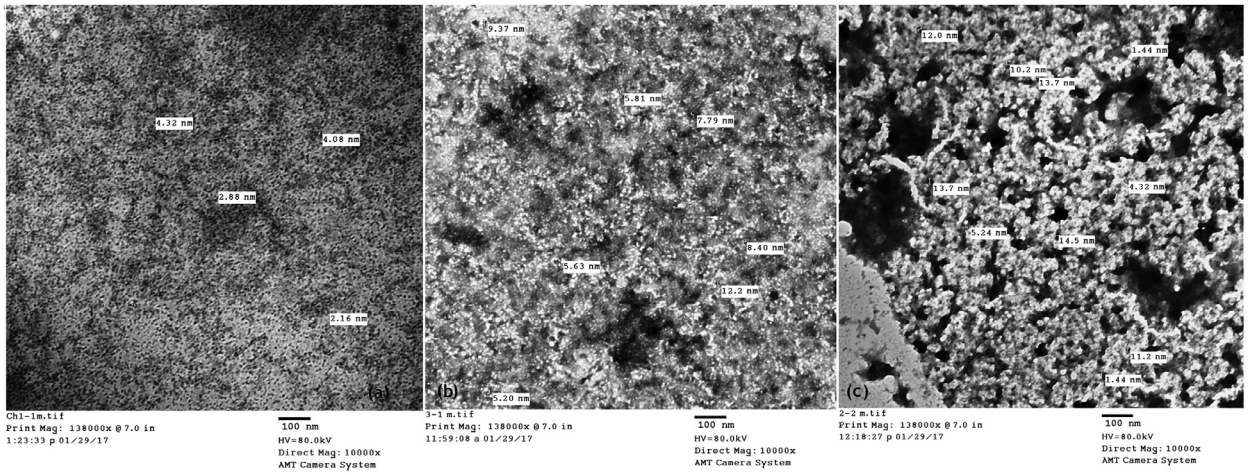

Figure 3 TEM images of (a) nano-chitosan, (b) iron nanoparticles biosynthesized using a *Ulva fasciata* extract, and (c) iron nanoparticles biosynthesized using an *Avicennia marina* leaf extract.

Table 1 AUs of the different extracts and nanoparticles.

Composite	Seawater community*	*Escherichia coli*	*Staphylococcus aureus*
Ulva fasciata extract only	1.8	—	—
Avicennia marina extract only	—	—	1.8
Iron nanoparticles + *Ulva fasciata* extract	2.3	4.0	4.0
Iron nanoparticles + *Avicennia marina* extract	3.4	2.3	3.4
Chitosan composite	1.8	—	1.8

* This sample was collected from the Eastern Harbor of Alexandria, Egypt, for isolating the seawater community.

Table 2 Numbers of recorded fouling species on the different test panels of the iron frames after being immersed for different periods in the water of the Eastern Harbor of Alexandria.

Frame	Iron frame Iafter more than 2 months			Iron frame IIafter more than 4 months			Iron frame IIIafter around 7 months		
Test	PVC	Wood	Steel	PVC	Wood	Steel	PVC	Wood	Steel
Control	3	7	3	15	14	14	23	17	21
1A	1	2	4	10	8	6	17	14	15
1B	3	1	3	10	8	8	13	9	11
1C	3	1	1	9	9	8	11	5	14
2A	1	3	4	5	6	10	19	12	10
2B	3	1	4	10	7	9	12	12	12
2C	5	3	4	6	6	12	20	11	13
3A	5	7	4	7	6	12	13	8	11
3B	4	2	3	6	7	8	8	12	14
3C	3	4	4	8	4	6	7	14	10

same inhibition value against both the bacterial community of the water taken from the Eastern Harbour and *S. aureus* (AU = 1.8), but shows no activity against *E. coli*. Moreover, these data exhibit that high AUs are detected for the iron nanoparticles with either algal or mangrove extracts. In particular, the iron + *U. fasciata* composite shows the highest AUs against both *E. coli* and *S. aureus* (AU = 4.0), while the iron + *A. marina* composite exhibits high AUs of 3.4 against both the seawater community and *S. aureus*.

3.5. Bacterial counts on the different treated panels

The marine bacterial populations that adhere to the PVC, wood, and steel panels submerged in seawater were estimated over a period of 10 days. For the different control panels under investigation, the bacterial count increased regularly for up to six days and then started to decrease sharply until the 10th day. The bacterial counts on the PVC control panel were 5×10^2, 3×10^3, and 1.2×10^3

cfu/cm^2 after 3, 6, and 10 days, respectively. For wood control, these values were 5×10^2, 3.2×10^3, and 1.4×10^3 cfu/cm^2 after 3, 6, and 10 days, and for steel control, they were 5×10^2, 7.1×10^3, and 1.6×10^3 cfu/cm^2 after 3, 6, and 10 days, respectively. However, the observed bacterial counts on different treated panels were rather lower than their counts on the controls ($p < 0.05$). There were variations in each treatment group and between different treatments. Generally, the bacterial count increased gradually until fouling appeared. So, the suppression percentages (%) detected by different biocides along the investigation period were calculated to express their antibacterial activity. The suppression % ranges from 64.3 to 100, but in most treatments, the values were ~97%, as shown in Figure 4.

3.6. Fouling community

After more than two months of immersion, the iron frame (I) was the first sample frame to be retrieved from the Eastern Harbour, upon which 15 marine fouling species were observed, including one Hydroid, four Bryozoa, three Polychaeta, two Barnacles, one Tanaidacea, and four Amphipoda species. Nine species were collected from the control panels. For the treated test panels, the number of recorded marine fouling varied according to the antifouling compounds used and their concentrations, as well as the type of substrate (Table 2, Figure 5).

It is evident that, for the control panels, the PVC panel was fouled by one Hydroid, one Polychaete, and one Barnacle species, the wood panel by three Bryozoa, one Polychaete, one Tanaidacea, and two Amphipoda species, and the steel panel by two Bryozoa and one Polychaete species. With respect to the treated test panels, only one species was recorded on PVC panels, which were coated with paints 1A and 2A. One species was observed on both the wood and steel panels coated with paint 1C.

Meanwhile, after more than four months of immersion, twenty marine fouling species were collected on iron frame II, including one Hydroid, eight Bryozoa, one Polychaete, four Barnacles, one Tanaidacea, and five Amphipoda species. Seventeen species were collected on the control test panels. The recorded marine fouling species were also diversified on the treated test panels (Table 2, Figure 6). With respect to the control panels; it was noticed that fifteen fouling species were settled on the control PVC panel, as well as fourteen species on both wood and steel panels, while the marine fouling species settled on the coated panels with different antifouling agents; only five species were recorded on PVC panel coated with paint 2A. Moreover, four species on wood, and six species on steel panels coated with paint 3C.

After around seven months of immersion, twenty-nine marine fouling species were collected on iron frame III, including two algae, five Bryozoa, five Polychaetes, four Barnacles, one Tanaidacea, three Isopoda, six Amphipoda, one Decapoda, and two Ascidia species. Meanwhile, twenty-six fouling species settled on the control test panels. On the other hand, the treated test panels also showed variable numbers of settled fouling species (Table 2, Figure 7).

The results of the iron frame (III) showed that for the control panels; the PVC test panel was fouled by 23 species, the wood by 17 species, and the steel by 21 species. While

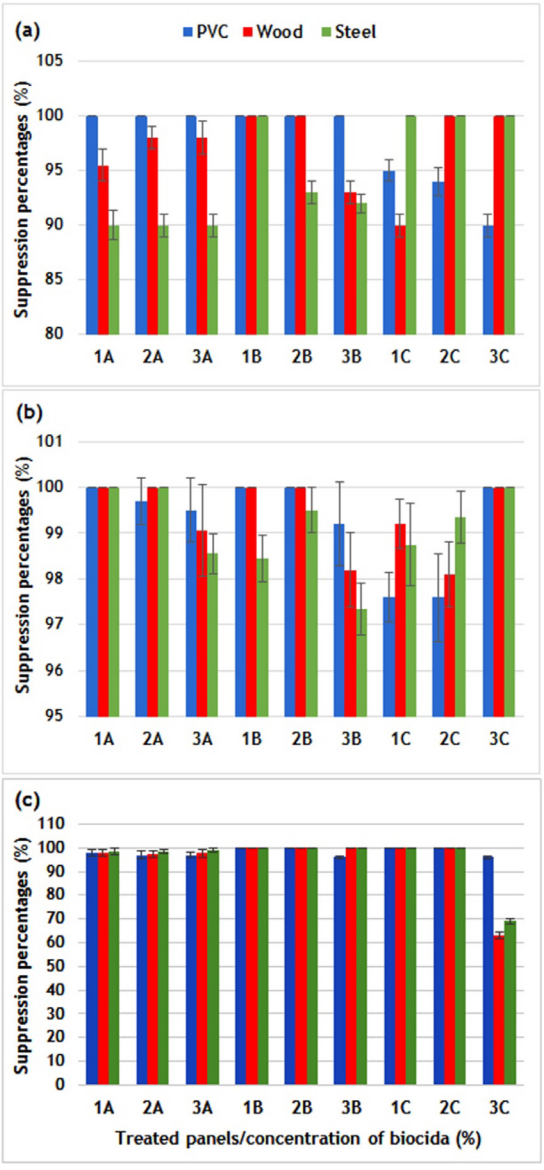

Figure 4 Suppression percentages (%) ± S.D. of the bacterial films by the different biocides after (a) 3 days, (b) 6 days, and (c) 10 days. 1A, 2A, and 3A contain 20%, 40%, and 60% nano-chitosan, respectively. 1B, 2B, and 3B contain 20%, 40%, and 60% *Ulva fasciata* extract. 1C, 2C, and 3C contain 20%, 40%, and 60% *Avicennia marina* extract; (n = 3).

for the treated test panels; only five species were recorded on a wood panel coated with paint 1C, seven, and ten species were observed on PVC and steel panels coated with paint 3C, respectively.

However, the lists of all recorded fouling taxa on different test panels, during various immersion periods, are provided in the supplementary tables (2–4).

3.7. Statistical results

Based on the number of settled fouling species as a dependent variable, the two-way ANOVA test indicated that

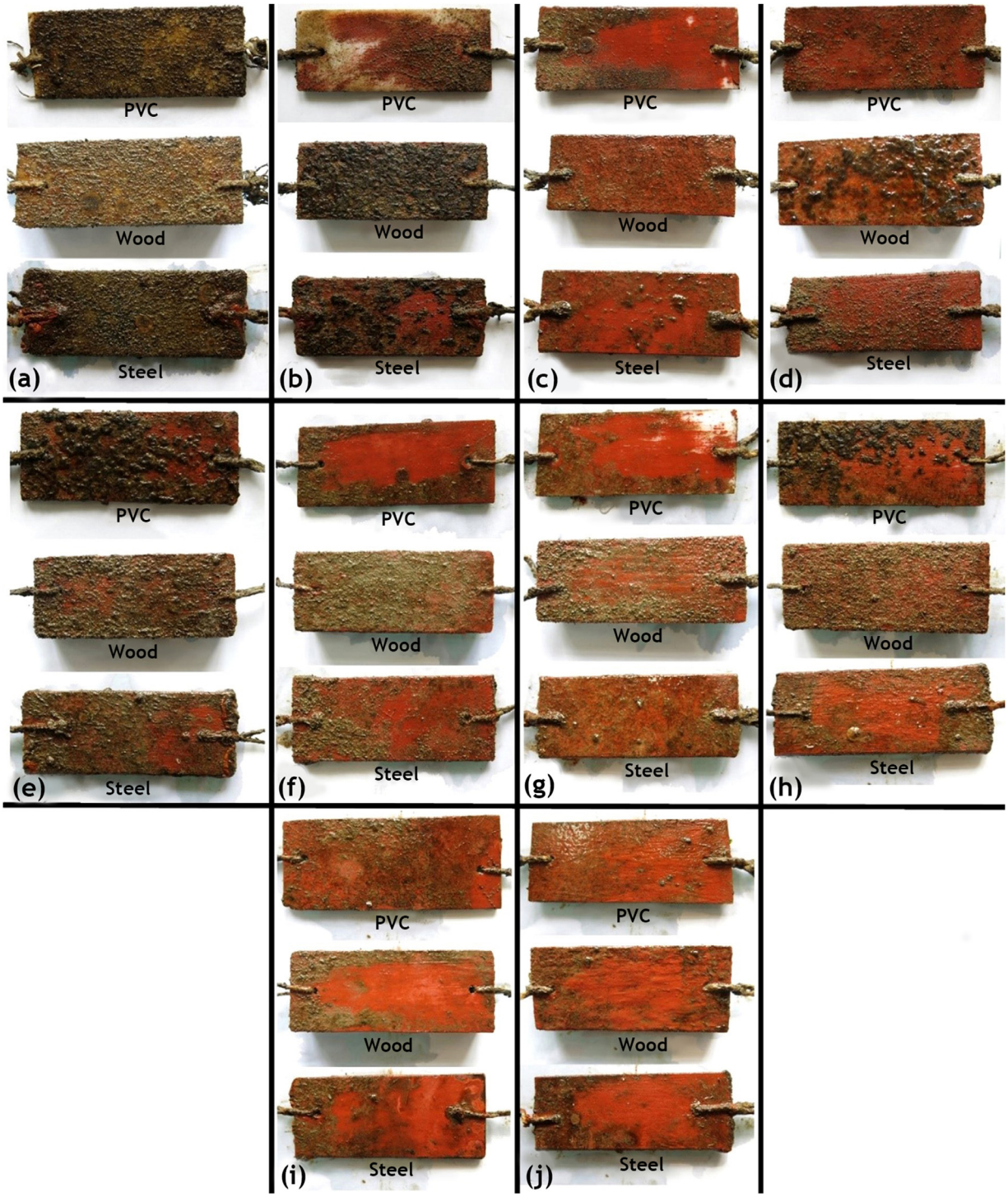

Figure 5 Biofouling species collected on the control and treated test panels of frame I, (a) Control, (b) 1A, (c) 1B, (d) 1C, (e) 2A, (f) 2B, (g) 2C, (h) 3A, (i) 3B, and (j) 3C.

there is a significant difference between durations i.e. 2, 4, and 7 months (Table 3). Results of the Post hoc test (Tukey HSD) indicated a higher number of settled fouling species during longer periods of exposure whenever, the maximum number of species is recorded in 7 months' duration which was significantly higher than the 2 months (10.78*) and the 4 months (4.64*) durations (Table 4). In addition, there is another significant difference between different compound concentrations and control. It is obvious from the estimated marginal means of the dependent variable (Figure 8) that the contrary effects of all compounds are more evident during longer periods (4 and 7-month durations) than the short one (2 months). Moreover, the extract of mangrove leaves *Avicennia marina* (compound C) was the most effec-

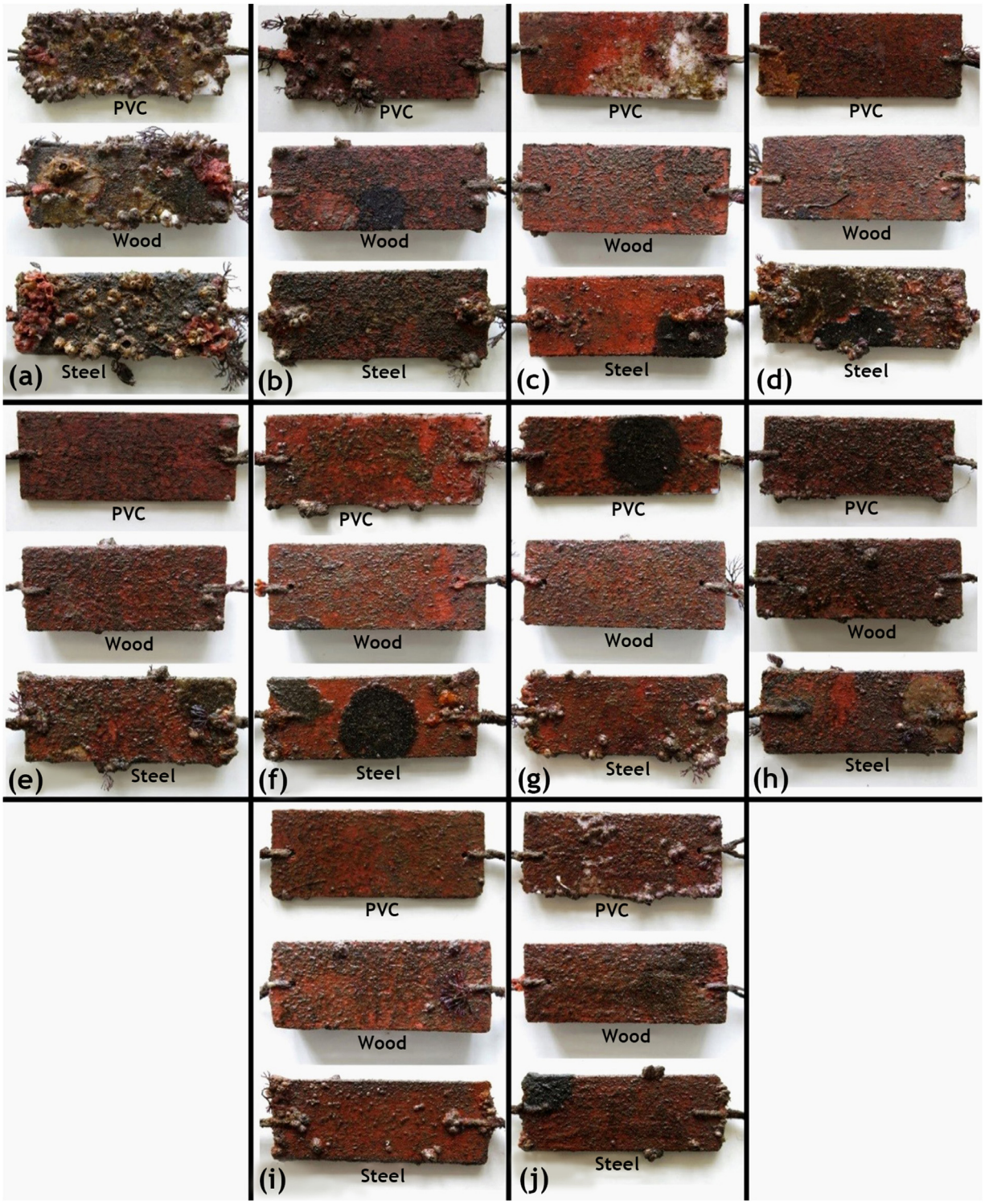

Figure 6 Biofouling species collected on the control and treated test panels of frame II, (a) Control, (b) 1A, (c) 1B, (d) 1C, (e) 2A, (f) 2B, (g) 2C, (h) 3A, (i) 3B, and (j) 3C.

tive compound as an antifouling agent through different durations. Results of the Post hoc test (Tukey HSD) indicated that the maximum inhibitory effects were recorded with 3C (−6.44*) and 1C (−6.33*) which were significantly less than the control.

4. Discussion

Marine biofouling is the term given to the accumulation of microorganisms, plants, algae, and small invertebrates on surfaces that are submerged in water. In the process of bio-

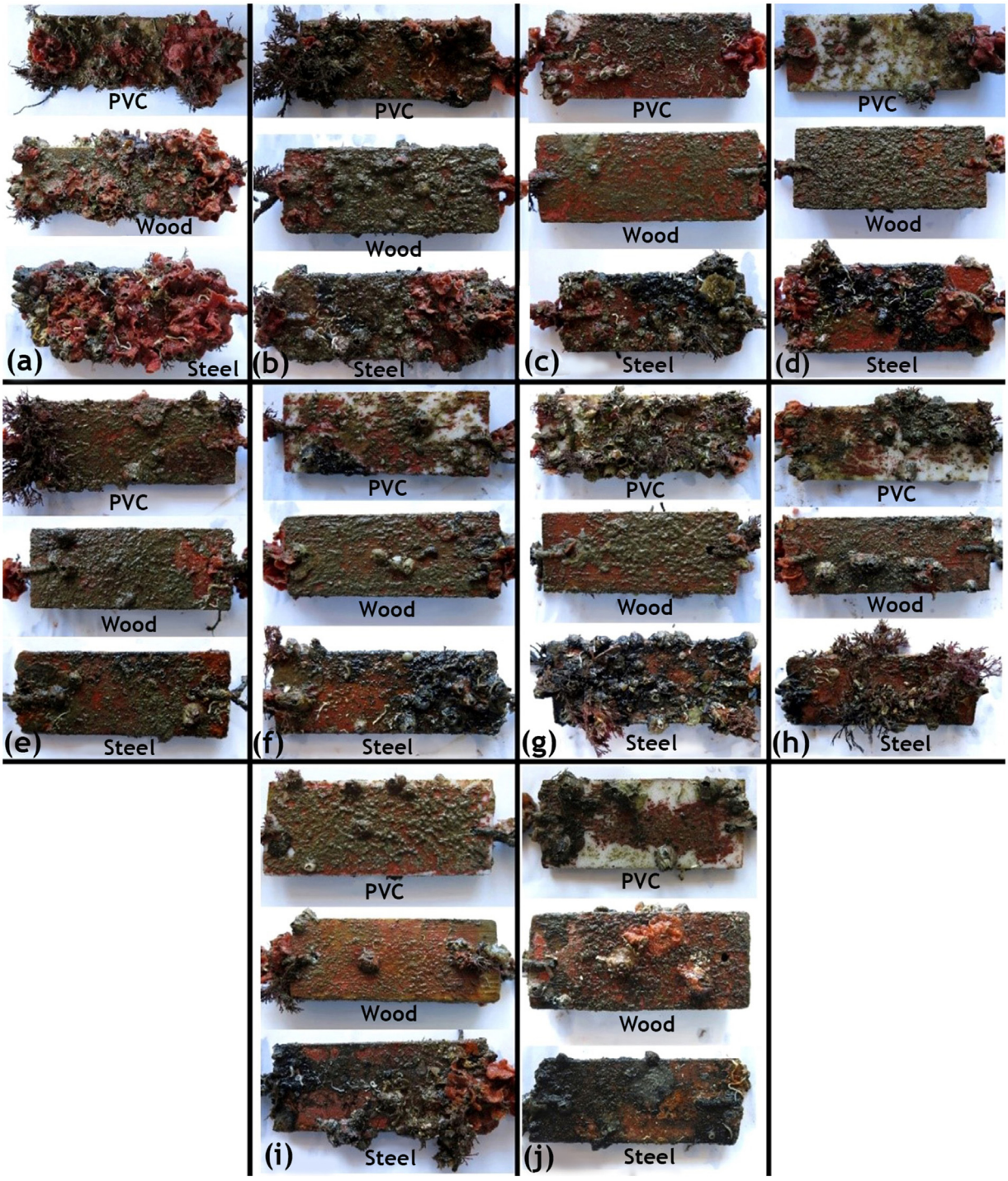

Figure 7 Biofouling species collected on the control and treated test panels of frame III, (a) Control, (b) 1A, (c) 1B, (d) 1C, (e) 2A, (f) 2B, (g) 2C, (h) 3A, (i) 3B, and (j) 3C.

fouling, a biofilm first forms, where one of the critical factors that affect its development is the feedwater quality, in terms of temperature, pH, DO content, and the presence of organic and inorganic nutrients. Once a microorganism finds an environment to which it is suited, growth proceeds, unless the conditions in the system become too inhospitable (Qian et al., 2003). In temperate regions (such as in Egypt), marine fouling is a common phenomenon, where the relatively high water temperature is the principal factor responsible for enhancing the breeding periods and increase the growth rates of fouling organisms (Rascio, 2000).

The hulls of ships are painted to keep fouling from 481 undesirable marine organisms under control (Chambers et al., 2006). However, there is evidence that some paints are poisonous and can undesirably affect non-target living organisms. Thus, the development of non-toxic

Table 3 Results of the two-way ANOVA test.

Tests of Between-Subjects Effects
Dependent Variable: Number of fouling species

Source	Type III Sum of Squares	df	Mean Square	F	Sig.
Corrected Model	3031.583[a]	29	104.537	20.216	.000
Intercept	6501.440	1	6501.440	1257.303	.000
Duration	1526.595	2	763.298	147.613	.000
Concentration	642.694	9	71.410	13.810	.000
Duration* Concentration	284.500	18	15.806	3.057	.000
Error	403.333	78	5.171		
Total	12237.000	108			
Corrected Total	3434.917	107			

[a] R Squared = .883 (Adjusted R Squared = .839).

Table 4 Results of Post Hoc test (Tukey test) among durations.

Multiple Comparisons
Dependent Variable: Number of fouling species
Tukey HSD

(I) Duration	(J) Duration	Mean Difference (I-J)	Std. Error	Sig.	95% Confidence Interval	
					Lower Bound	Upper Bound
2	4 months	-6.14*	.536	.000	-7.42	-4.86
months	7 months	-10.78*	.536	.000	-12.06	-9.50
4	2 months	6.14*	.536	.000	4.86	7.42
months	7 months	-4.64*	.536	.000	-5.92	-3.36
7	2 months	10.78*	.536	.000	9.50	12.06
months	4 months	4.64*	.536	.000	3.36	5.92

Based on observed means.
The error term is Mean Square(Error) = 5.171.
* The mean difference is significant at the .05 level.

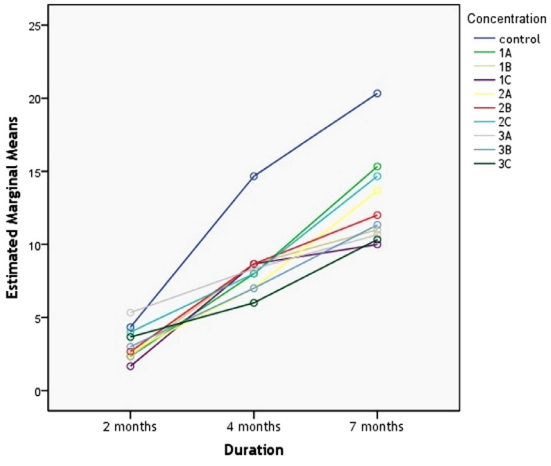

Figure 8 Estimated marginal means of the number of settled fouling species on control and different concentration of various paints.

coatings that can successfully control biofouling is of high priority. Numerous natural plants and other organisms, such as coral, sponges, seaweed, and land plants, exhibit efficient antifouling behavior (Negm et al., 2018). Studies are currently underway into the development of materials that can enable these to be combined with the polymeric matrices of antifouling paints, with the end goal of developing a product that does not leach out harmful compounds in water, and thus, does not pollute the environment (Almeida et al., 2007).

At the National Institute of Oceanography and Fisheries (NIOF, Egypt), several crude extracts have been prepared from marine organisms and resources, and their potentiality against microbial pathogens, especially *S. aureus*, has been tested. For instance, Botros Tadros et al. (2009) examined the free lipid *U. lactuca* on glass panels immersed in a medium inoculated with *S. aureus* ATCC 6538 as a model organism for biofilm formation. The results showed that 5% of the free lipid *U. lactuca* suppressed 82% of *S. aureus* (ATCC 6538) attached to the glass panels and 85% of free *S. aureus* in the medium. Recently, Negm et al. (2018) used an environmentally friendly method to synthesize silver nanoparticle (AgNP)-embedded biological marine extracts (BMEs) from four species of marine algae (*U. fasciata*, *Grateloupia* sp., *Pterocladiella capillacea*, and *Corallina mediterranea*). They evaluated their antibacterial properties and anti-biofilm activity against indicator strains and 506 bacterial communities, and observed positive antibacterial activity in the range 2.4—23.6 AU. It was determined that

an aqueous extract of *Ulva fasciata* was the most efficient among the different algal species screened for use in the green synthesis of AgNPs/BMEs.

In the in situ experiments conducted in this study, attention has been focused on both wood and steel panels that representing the main materials used in various boats and vessels.

It should be noted that the number of marine fouling species settled on the panels was affected by both the duration of the panel immersion and the season in which the immersion was conducted (Brown and Swearingen, 1998). Generally, at temperate latitudes, heavy fouling might occur in the summer, but during the cold winter period, little growth occurs. In total, nine marine fouling species were collected on the control test panels of the iron frame (I), which was immersed for more than two months in seawater. This number increased to 17 on the iron frame (II), which was immersed in seawater for more than four months. Additionally, 26 marine fouling species were collected on the iron frame (III), which had been immersed in seawater for around seven months. The two-way ANOVA test confirmed that there is a significant difference between durations with more settled fouling species during longer periods of exposure ($p < 0.05$).

The number of barnacles that settle on the tested steel panels is important in selecting the most favorable type of antifouling paint, as these creatures corrode metal surfaces (Shide, 1989). In this work, after four months of immersion, the steel panel coated with paint 3C contained only four barnacles, constituting ~5% of the total barnacles found on the control panel. In addition, the steel panel coated with paint formulation 3C showed only one barnacle attached to it, making up to ~2% of the total barnacles found on the control panel after around seven months of immersion. These results confirmed the great importance of using mangrove extract nanoparticles as an antifouling agent.

In accordance with our results, Pelletier et al. (2009) estimated the antifouling activity of chitosan in a marine environment, showing that a coating with 20% chitosan exhibited antibacterial activity after 14 days of immersion in an estuary, while that with 5% chitosan exhibited no antifouling activity. It is well-known that the cationic amine group in the chitosan molecule plays a major role in its antimicrobial activity, as it forms electrostatic interactions with anionic groups on the cell membrane of bacterial cells, which eventually lead to cell death (Alishahi and Aïder, 2012). This explains why chitosan antifouling efficiency increases by increasing its concentration in the paint.

In general, the promising results of the nanoparticle biosynthesized extracts from (chitosan, *U. fasciata*, and mangrove leaf *A. marina*), can be attributed to the antimicrobial activity of the bioactive compounds contained in the extracts, such as polyunsaturated fatty acids, phenols, alcohols, amines, amides, ammonium, flavonoids, terpenoids, alkaloids, quinones, sterols, polyketides, phlorotannins, polysaccharides, glycerols, peptides, and lipids. All these compounds prevent the formation of biofilm on immersed panels and hence inhibit or decrease the rate of fouling.

Traditionally, mangrove plant extracts are widely used as antimicrobial agents (Shamsuddin et al., 2013) and exhibit significant antifouling activity (Chen et al., 2008). Many studies have shown their specific activity in inhibiting the growth of virulent strains of bacterial pathogens (Abou-Elela et al., 2009; Sahoo et al., 2012).

Avicennia marina contains a mixture of fatty acids such as alpha-linolenic, palmitic, stearic, lauric, myristic, and oleic acids, as well as their derivatives (Selvin et al., 2009). It has been confirmed that *A. marina* also contains terpenoids (Azuma et al., 2002), triterpenoids, and alkaloids (Abeysinghe, 2010; Chen et al., 2008; Ravikumar et al., 2010). Moreover, Sahoo et al. (2012) revealed that mangrove plants contain saponins, glycosides, tannins, flavonoids, phenols, and volatile oils in their leaves. Therefore, these natural biocides are bioactive compounds and ideal for the development of biodegradable antifouling materials (Selvin et al., 2009).

The superior efficiency of the extract C nanoparticle additive as an antifouling agent, compared to extracts A and B, can be attributed to it containing polyphenols and ammonium compounds, very high concentrations of alcohol, and the presence of both aromatic and aliphatic amide and amide derivatives. Hydroxyl, carboxyl, and amino groups were found to exist in these compounds, as presented in its IR spectrum, showing that extract C has high antimicrobial activity. In addition, polyphenols act as a strong reducing agent of the metal (nano-iron), resulting in a remarkable increase in its antimicrobial activity (Cetin-Karaca, 2011). The presence of aliphatic, branched, and aromatic amides confirm the presence of enzymes that biologically control and prevent biofilm formation, hence reducing the development of fouling. Moreover, the presence of ammonium groups, identified in the IR spectrum, confirms the antimicrobial activity of the extract (Kabara et al., 1972).

The strong activity of extract C can also be explained by looking at the ionic state of the compounds, as it contains both anions (oxidizing compounds), such as fatty acids, amide derivatives, and N-methylated derivatives of amine compounds, and cationic compounds (non-oxidizing compounds), such as ammonium, aldehydes, alkaloids, terpenoids, and flavonoids, in amounts and greater variability than those in extracts A and B. The mechanism of action of anionic compounds in antifouling can be attributed to their efficiency as antimicrobial agents for a wide spectrum of gram-positive and negative bacteria. Only anionic compounds can completely diffuse through the cell membrane and cause lysis of the protoplast, and promote the complete dissolving of protein moieties, such as the lipoprotein of the membrane. The mode of action of cationic compounds in fouling prevention is limited to gram-positive bacteria, as they react with the phosphotidic, phosphatidic, and lipid components of the cytoplasmic membrane, disturbing its permeability (Alves et al., 2013; Farhadi et al., 2019).

In addition, most compounds in extract (C) are hydrophilic, such as alcohols, phenols, carboxylic compounds, ammonium, amides, branched amines.45, and alkyl halides. This means that the surface covered with paints mixed with extract C is less fouled than that coated with B (which contains both hydrophilic and hydrophobic compounds) and much less than those coated with extract A, in which most of its compounds are hydrophobic. The observed results reflect the constituents of each extract, as a hydrophobic surface may cause other non-polar or hydrophobic compounds to be adsorbed onto the surface, resulting in biofouling.

5. Conclusions

To develop active biocides that can control micro- and macrofouling, three natural resources (chitosan, *Ulva fasciata*, and *Avicennia marina* leaves) were immobilized with different nanoparticles, and then mixed with 20%, 40%, and 60% by weight of the prepared paint formulation, to produce nine paints. In situ experiments in the water of the Eastern Harbour of Alexandria, Egypt, were conducted to test the effectiveness of the coating as antifouling agents. The experimental results showed that no sample was completely resistant to fouling, but surfaces coated with compound C (containing the *A. marina* leaf extract) were the least fouled and could effectively resist both micro- and macro-fouling during different immersion intervals.

Declaration of competing interest

This manuscript is original, not under consideration elsewhere and approved by all authors and institutions prior to submission.

The authors declare that they have no known competing financial interests or personal relationships that could have appeared to influence the work reported in this paper.

Acknowledgements

This project was financially supported by the Marine Environment Division, National Institute of Oceanography and Fisheries, NIOF, Egypt [grant number MED 0004 — 2018]. Title of the project "Nanochitosan composites as antibiofouling agents in vitro and in situ".

Supplementary materials

Supplementary material associated with this article can be found, in the online version, at https://doi.org/10.1016/j.oceano.2021.08.004.

References

Abdel-Latif, H.H., Shams El-Din, N.G., Ibrahim, H.A.H., 2018. Antimicrobial activity of the newly recorded red alga *Grateloupia doryphora* collected from the Eastern Harbor, Alexandria, Egypt. J. Appl. Microbiol. 125, 1321—1332. https://doi.org/10.1111/jam.1405

Abdel Aleem, A., 1993. The Marine Algae of Alexandria, Egypt, 138 pp.

Abeysinghe, P.D., 2010. Antibacterial activity of some medicinal mangroves against antibiotic resistant pathogenic bacteria. Indian J. Pharm. Sci. 72, 167—172. https://doi.org/10.4103/0250-474X.65019

Abou-Elela, G.M., 1994. Studies on the settlement of marine bacteria and its response to some coatings on artificial substrata in Alexandria Eastern Harbour. M.Sc. thesis, Faculty of Science, Alexandria University, 156 pp.

Abou-Elela, G.M., El-Sersy, N.A., El-Shenawy, M.A., Abd-Elnabi, H., Ibrahim, H.A.H., 2009. Bio-Control of Vibrio fluvialis in Aquaculture by Mangrove (*Avicennia marina*) Seeds Extracts. Res. J. Microbiol. 4, 38—48. https://doi.org/10.3923/jm.2009.38.48

Ali, S.W., Rajendran, S., Joshi, M., 2011. Synthesis and characterization of chitosan and silver loaded chitosan nanoparticles for bioactive polyester. Carbohydr. Polym. 83, 438—446. https://doi.org/10.1016/j.carbpol.2010.08.004

Alishahi, A., Aïder, M., 2012. Applications of Chitosan in the Seafood Industry and Aquaculture: A Review. Food Bioprocess Technol. 5, 817—830. https://doi.org/10.1007/s11947-011-0664-x

Almeida, E., Diamantino, T.C., de Sousa, O., 2007. Marine paints: The particular case of antifouling paints. Prog. Org. Coatings 59, 2—20. https://doi.org/10.1016/j.porgcoat.2007.01.017

Alves, M.J., Ferreira, I.C.F.R., Froufe, H.J.C., Abreu, R.M.V, Martins, A., Pintado, M., 2013. Antimicrobial activity of phenolic compounds identified in wild mushrooms, SAR analysis and docking studies. J. Appl. Microbiol. 115, 346—357. https://doi.org/10.1111/jam.12196

Azuma, H., Toyota, M., Asakawa, Y., Takaso, T., Tobe, H., 2002. Floral scent chemistry of mangrove plants. J. Plant Res. 115, 47—53. https://doi.org/10.1007/s102650200007

Bather, J.M., Riley, J.P., 1954. The chemistry of the irish sea. Part I. The sulphate-chlorinity ratio. ICES J. Mar. Sci. 20, 145—152. https://doi.org/10.1093/icesjms/20.2.145

Bellan-Santini, D., Diviacco, G., Krapp-Schickel, G., Ruffo, S., 1989. The Amphipoda of the Mediterranean. Part 2. Gammaridea (Haustoriidae to Lysianassidae). Mémoires de l' Institut Océanographique, Monaco, 365—576.

Bhadury, P., Wright, P.C., 2004. Exploitation of marine algae: Biogenic compounds for potential antifouling applications. Planta 219, 561—578. https://doi.org/10.1007/s00425-004-1307-5

Botros Tadros, A., Abdalla Ibrahim, H., Ramzy Zaki, H., Mahmoud El-Naggar, M., Eid Abbas, A., 2009. Suppressive effect of coated surfaces contain *Ulva lactuca* free lipid on Staphylococcus aureus ATCC 6538. Egypt. J. Aquat. Res. 35, 405—412.

Brown, K.M., Swearingen, D.C., 1998. Effects of seasonality, length of immersion, locality and predation on an intertidal fouling assemblage in the Northern Gulf of Mexico. J. Exp. Mar. Bio. Ecol. 225, 107—121. https://doi.org/10.1016/S0022-0981(97)00217-7

Campbell, A.C., Gorringe, R., Nicholls, J. , 1982. The Hamlyn Guide to the Flora and Fauna of the Mediterranean Sea. Hamlyn, London, New York, Sydney, Toronto, 321 pp.

Cetin-Karaca, H., 2011. Evaluation of Natural Antimicrobial Phenolic Compounds against Food borne Pathogens. Faculty of Agriculture, University of Kentucky M.Sc. Thesis, 652 pp.

Chambers, L.D., Stokes, K.R., Walsh, F.C., Wood, R.J.K., 2006. Modern approaches to marine antifouling coatings. Surf. Coatings Technol. 201, 3642—3652. https://doi.org/10.1016/j.surfcoat.2006.08.129

Chen, J.J., Fei, D.Q., Chen, S.G., Gao, K., 2008. Antimicrobial triterpenoids from *Vladimiria muliensis*. J. Nat. Prod. 71, 547—550. https://doi.org/10.1021/np070483l

De Marco, B.A., Rechelo, B.S., Tótoli, E.G., Kogawa, A.C., Salgado, H.R.N., 2019. Evolution of green chemistry and its multidimensional impacts: A review. Saudi Pharm. J. 27, 1—8. https://doi.org/10.1016/j.jsps.2018.07.011

Dobretsov, S., Rittschof, D., 2020. Love at first taste: induction of larval settlement by marine microbes. IJMS 21, 731. https://doi.org/10.3390/ijms21030731

Farhadi, F., Khameneh, B., Iranshahi, M., Iranshahy, M., 2019. Antibacterial activity of flavonoids and their structure—activity relationship: An update review. Phyther. Res. 33, 3—40. https://doi.org/10.1002/ptr.6208

Hadfield, M.G., 2011. Biofilms and marine invertebrate larvae: what bacteria produce that larvae use to choose settlement sites. Ann. Rev. Mar. Sci. 3, 453—470. https://doi.org/10.1146/annurev-marine-120709-142753

Hurst, G.A., 2020. Systems thinking approaches for international green chemistry education. Curr. Opin. Green Sustain. Chem. 21, 93—97. https://doi.org/10.1016/j.cogsc.2020.02.004

Kabara, J.J., Conley, A.J., Truant, J.P., 1972. Relationship of chemical structure and antimicrobial activity of alkyl amides and amines. Antimicrob. Agents Chemother. 2, 492—498. https://doi.org/10.1128/AAC.2.6.492

Kolanjinathan, K., Ganesh, P., Saranraj, P., 2014. Pharmacological Importance of Seaweeds: A Review. World J. Fish Mar. Sci. 6, 1—15. https://doi.org/10.5829/idosi.wjfms.2014.06.01.76195

Kong, M., Chen, X.G., Xing, K., Park, H.J., 2010. Antimicrobial properties of chitosan and mode of action: A state of the art review. Int. J. Food Microbiol. 144, 51—63. https://doi.org/10.1016/j.ijfoodmicro.2010.09.012

Krishnan, M., Sivanandham, V., Hans-Uwe, D., Murugaiah, S.G., Seeni, P., Gopalan, S., Rathinam, A.J., 2015. Antifouling assessments on biogenic nanoparticles: A field study from polluted offshore platform. Mar. Pollut. Bull. 101, 816—825. https://doi.org/10.1016/j.marpolbul.2015.08.033

Lamsal, K., Kim, S.W., Jung, J.H., Kim, Y.S., Kim, K.S., Lee, Y.S., 2011. Application of silver nanoparticles for the control of Colletotrichum species in vitro and pepper anthracnose disease in field. Mycobiology 39, 194—199. https://doi.org/10.5941/MYCO.2011.39.3.194

Mahdavi, M., Namvar, F., Ahmad, M.Bin, Mohamad, R., 2013. Green biosynthesis and characterization of magnetic iron oxide (Fe_3O_4) nanoparticles using seaweed (*Sargassum muticum*) aqueous extract. Molecules 18, 5954—5964. https://doi.org/10.3390/molecules18055954

Mohy El-Din, S.M., El-Ahwany, A.M.D., 2015. Bioactivity and phytochemical constituents of marine red seaweeds (*Jania rubens, Corallina mediterranea and Pterocladia capillacea*). J. Taibah Univ. Sci. 10, 471—484. https://doi.org/10.1016/j.jtusci.2015.06.004

Negm, M.A., Ibrahim, H.A.H., Shaltout, N.A., Shawky, H.A., Abdel—mottaleb, M.S., Hamdona, S.K., 2018. Green Synthesis of Silver nanoparticles Using Marine Algae Extract and Their Antibacterial Activity. Middle East J. Appl. Sci. 8, 957—970.

Parsons, T.R., Maita, Y., Lalli, C.M., 1984. A Manual of Chemical & Biological Methods for Seawater Analysis. Pergamon Press, Oxford and New York, 173 pp. https://doi.org/10.1016/c2009-0-07774-5

Patil, M.P., Kim, G.-D., 2017. Eco-friendly approach for nanoparticles synthesis and mechanism behind antibacterial activity of silver and anticancer activity of gold nanoparticles. Appl. Microbiol. Biotechnol. 101, 79—92. https://doi.org/10.1007/s00253-016-8012-8

Patil, M.P., Kim, G—D, 2018. Marine microorganisms for synthesis of metallic nanoparticles and their biomedical applications. Colloids and Surfaces B: Biointerfaces 172, 487—495. https://doi.org/10.1016/j.colsurfb.2018.09.007

Pelletier, É., Bonnet, C., Lemarchand, K., 2009. Biofouling growth in cold estuarine waters and evaluation of some chitosan and copper anti-fouling paints. Int. J. Mol. Sci. 10, 3209—3223. https://doi.org/10.3390/ijms10073209

Peng, L-H., Liang, X., Chang, R-H., Mu, J-Y., Chen, H-E., Yoshida, A., Osatomi, K., Yang, J-L., 2020. A bacterial polysaccharide biosynthesis-related gene inversely regulates larval settlement and metamorphosis of *Mytilus coruscus*. Biofouling 36 (7), 753—765 https://doi:1080/08927014.2020.1807520.

Puvvada, Y.S., Vankayalapati, S., Sukhavasi, S., 2012. Extraction of chitin from chitosan from exoskeleton of shrimp for application in the pharmaceutical industry. Int. Curr. Pharm. J. 1, 258—263. https://doi.org/10.3329/icpj.v1i9.11616

Qi, L., Xu, Z., Jiang, X., Hu, C., Zou, X., 2004. Preparation and antibacterial activity of chitosan nanoparticles. Carbohydr. Res. 339, 2693—2700. https://doi.org/10.1016/j.carres.2004.09.007

Qian, P.Y., Thiyagarajan, V., Lau, S.C.K., Cheung, S.C.K., 2003. Relationship between bacterial community profile in biofilm and attachment of the acorn barnacle *Balanus amphitrite*. Aquat. Microb. Ecol. 33, 225—237. https://doi.org/10.3354/ame033225

Ramkumar, V.S., Pugazhendhi, A., Gopalakrishnan, K., Sivagurunathan, P., Saratale, G.D., Dung, T.N.B., Kannapiran, E., 2017. Biofabrication and characterization of silver nanoparticles using aqueous extract of seaweed Enteromorpha compressa and its biomedical properties. Biotechnol. Reports 14, 1—7. https://doi.org/10.1016/j.btre.2017.02.001

Rascio, V.J.D., 2000. Antifouling coatings: Where do we go from here. Corros. Rev. 18, 133—154. https://doi.org/10.1515/CORRREV.2000.18.2-3.133

Ravikumar, S., Gnanadesigan, M., Suganthi, P., Ramalakshmi, A., 2010. Antibacterial potential of chosen mangrove plants against isolated urinary tract infectious bacterial pathogens. Int. J. Med. Med. Sci. 2, 94—99.

Riedl, R., 1970. Fauna und Flora der Adria. Verlag Paul Parey, Hamburg und Berlin, 702 pp. https://doi.org/10.1007/BF02285734

Sahoo, G., Mulla, N.S.S., Ansari, Z.A., Mohandass, C., 2012. Antibacterial activity of mangrove leaf extracts against human pathogens. Indian J. Pharm. Sci. 74, 348—351. https://doi.org/10.4103/0250-474X.107068

Selvin, J., Manilal, A., Sujith, S., Kiran, G.S., Shakir, C., 2009. Biopotentials of Mangroves Collected from the Southwest Coast of India. Glob. J. Biotechnol. Biochem. 4, 59—65.

Shamsuddin, A.A., Najiah, M., Suvik, A., Azariyah, M.N., Kamaruzzaman, B.Y., Effendy, A.W., Akbar John, B., 2013. Antibacterial properties of selected mangrove plants against vibrio species and its cytotoxicity against Artemia salina. World Appl. Sci. J. 25, 333—340. https://doi.org/10.5829/idosi.wasj.2013.25.02.688

Shah, M., Fawcett, D., Sharma, S., Tripathy, S.K., Poinern, G.E.J., 2015. Green synthesis of metallic nanoparticles via biological entities. Materials 8, 7278—7308. https://doi.org/10.3390/ma8115377

Shi, D., Li, J., Guo, S., Han, L., 2008. Antithrombotic effect of bromophenol, the alga-derived thrombin inhibitor. J. Biotechnol. 136, 577—588. https://doi.org/10.1016/j.jbiotec.2008.07.1364

Shide, M., 1989. The corrosive effect of barnacles on low alloy steels. Chinese J. Oceanol. Limnol. 7, 271—273. https://doi.org/10.1007/BF02842617

Tang, Z.X., Qian, J.Q., Shi, L.E., 2007. Preparation of chitosan nanoparticles as carrier for immobilized enzyme. Appl. Biochem. Biotechnol. 136, 77—96. https://doi.org/10.1007/BF02685940

Tikhonov, V.E., Stepnova, E.A., Babak, V.G., Yamskov, I.A., Palma-Guerrero, J., Jansson, H.B., Lopez-Llorca, L.V, Salinas, J., Gerasimenko, D.V, Avdienko, I.D., Varlamov, V.P., 2006. Bactericidal and antifungal activities of a low molecular weight chitosan and its N-/2(3)-(dodec-2-enyl) succinoyl/-derivatives. Carbohydr. Polym. 64, 66—72. https://doi.org/10.1016/j.carbpol.2005.10.021

Venkatesan, J., Qian, Z.J., Ryu, B., Ashok Kumar, N., Kim, S.K., 2011. Preparation and characterization of carbon nanotube-grafted-chitosan — Natural hydroxyapatite composite for bone tissue engineering. Carbohydr. Polym. 83, 569—577. https://doi.org/10.1016/j.carbpol.2010.08.019

Wang, K.L., Wu, Z.H., Wang, Y., Wang, C.Y., Xu, Y., 2017. Mini-review: Antifouling natural products from marine microorganisms and their synthetic analogs. Mar. Drugs 15, 1—21. https://doi.org/10.3390/md15090266

Zabala, M., Maluquer, P., 1988. Illustrated keys for the classification of Mediterranean Bryozoa. Treballs — Mus. Zool. 4, 1—294.

Zbakh, H., Chiheb, H., Bouziane, H., Sánchez, V.M., Riadi, H., 2012. Antibacterial Activity of Benthic Marine Algae Extracts from the Mediterranean coast of Morocco. J. Microbiol. Biotechnol. Food Sci. 1, 219—228.